Impact of sea-ice bottom topography on the Ekman pumping

G. Castellani, R. Gerdes, M. Losch, C. Lüpkes

Abstract Sea-ice elevation profiles and thickness measurements have been collected during summer 2011 in the Central Arctic. These two different data sets have been combined in order to obtain surface and bottom topography of the sea-ice. From the bottom profile, the keels of ridges are detected. Then, a parameterization of oceanic drag coefficients that accounts for the keels depth and density is applied. The calculated oceanic drag coefficients are highly variable (between about $2 \cdot 10^{-3}$ and about $8 \cdot 10^{-3}$) within the range of observed values. In order to estimate the contribution of variable drag coefficients on the Ekman pumping, the calculated drag coefficients are used in a idealized model experiment, where sea ice is drifting at constant velocity on an ocean at rest. The resulting variations of the Ekman vertical velocity are in the same order of magnitude as for variable ice velocity at the surface. In most state-of-the-art general circulation models, the variations of drag coefficients are not taken into account. The simple experiment carried out in the present study suggests that neglecting this contribution can lead to an incorrect representation of the momentum exchange between ice and ocean and to an underestimation of the Ekman pumping, with consequences for the large scale ocean circulation.

Giulia Castellani
Alfred Wegener Institute Helmholtz Center for Polar and Marine Research, Bussestrasse 24, 27570, Bremerhaven, Germany e-mail: giulia.castellani@awi.de
Jacobs University, Bremen, Germany

Rüdiger Gerdes
Alfred Wegener Institute Helmholtz Center for Polar and Marine Research, Bussestrasse 24, 27570, Bremerhaven, Germany e-mail: ruediger.gerdes@awi.de

Martin Losch
Alfred Wegener Institute Helmholtz Center for Polar and Marine Research, Bussestrasse 24, 27570, Bremerhaven, Germany e-mail: martin.losch@awi.de

Christof Lüpkes
Alfred Wegener Institute Helmholtz Center for Polar and Marine Research, Bussestrasse 24, 27570, Bremerhaven, Germany e-mail: christof.luepkes@awi.de

1 Introduction

The sea ice in the Arctic Ocean has a surface and bottom topography that is characterized by many different scales from small hummocks and piles of ice to large ridges. A pressure ridge consists of a part that extends into the atmosphere (sail) and a part that extends into the ocean (keel).

The sails are usually above one meter, sometimes they can be as high as 2 m. In order to satisfy the hydrostatic equilibrium, the keels usually extend much deeper into the ocean and may reach depths of 30 m [17]. The formation of these topographic features depends on the ice motion. In particular, large pressure ridges are formed when the ice is exposed to strong convergence.

The main forces that govern the ice motion are the internal forces [21], the local winds and the ocean currents [24]. In the momentum balance equation that describes the ice motion, the interactions between air, ice and water are parameterized by drag coefficients. These drag coefficients must account for sea ice surface characteristics on the near-surface transport of momentum. The sea ice surface is spatially and temporally inhomogeneous and thus we can expect spatial and temporal variations of the drag coefficients as well.

Many studies addressed the dependence of the drag coefficients on the surface topography of the ice. In particular, for the atmospheric drag coefficients, parameterizations for numerical models have been developed (see, e.g., [3], [5], [13], [14], [15]). In these parameterizations the atmospheric drag coefficients are a function of surface characteristics of the ice (i.e., melt ponds, pressure ridges, floe edges). Only very few studies focused on the oceanic drag coefficients. Among these few, the studies by [22] and [23] relate the drag coefficients to the roughness of the ice, whereas in [12] the oceanic drag coefficients are expressed as a function of observable geometric parameters of the sea ice such as the depth of keels, the mean separation between ridges, and the floe edges.

The momentum transferred by wind or ice to the ocean is redistributed by vertical turbulent mixing from the surface to a certain depth. The layer with turbulence, that is where the vertical variations of the surface stress are not negligible, is called the *Ekman layer*. The fluxes of momentum lead to the formation of a velocity field in the surface layer of the ocean. Associated with the induced velocity is the vertical *Ekman pumping* (when directed upwards) or *Ekman suction* (when directed downwards). The Ekman pumping (suction) depends on the wind stress applied at the upper surface and represents the amount of volume pumped from below into (or from above out of) the Ekman layer. It was also shown ([18]) that variations in Ekman pumping affect the depth of the 34-isohaline with consequences for the entire ocean circulation. In most state-of-the-art global circulation models, the stress at the ice-ocean interface depends on the variability of the wind field, while variations in the drag coefficients are usually not taken into account. In the present study we calculate oceanic drag coefficients as function of observed ice topography. These drag coefficients are then used to illustrate the effects on Ekman pumping when only the spatial variations of the oceanic drag are considered.

2 Data and Methods

The data used for this study were collected by helicopter flights over the Arctic Ocean during a campaign with the ice breaker *RV Polarstern* in summer 2011. The map with the tracks along which the data have been collected is shown in figure 1.

During the campaign, two different types of data have been collected: sea-ice surface elevation profiles using a laser altimeter and sea-ice thickness using the so-called 'EM-bird'. The laser altimeter profiles are collected using a Riegel LD90-3100HS that was introduced in 2001. This instrument has a wavelength of 905 nm, a sampling frequency of 100 Hz and an accuracy of $\pm$ 1.5 cm. The point spacing is about 30-40 cm. The profiles recorded by the laser altimeter show an altitude variation due to the surface roughness of the ice and a variation, at a lower frequency, due to the movement of the helicopter. In order to remove this movement, a combination of low and high pass filters is used [8].

The 'EM-bird' is a device to measure the sea ice thickness directly using electromagnetic induction ([6], [7]). The EM-bird contains two coils for transmission and receptions of electromagnetic fields and can measure the distance between the instrument and the ice-ocean interface by using the electromagnetic field generated by induction in the conductive sea water. In addition, a laser altimeter (as described above) gives the distance of the instrument to the surface (ice or snow), hence the thickness is obtained by the difference between laser and EM measurements. The sea-ice thickness is sampled at 10 Hz, which leads to an average point spacing of $\sim$4 m. The footprint of the instrument is about 40 m ([11], [20]). Ice thickness samples thinner than 0.1 m are considered as open water. Since sea ice surface and underside profiles are recorded at the same time we can have a complete description of the ice topography on the surface and underneath the ice.

In order to obtain information about the bottom topography of the ice, in each point where both measurements are available, the thickness recorded with the EM-bird is subtracted from the filtered laser altimeter profiles. The spatial resolution is lower than the one for the upper surface (30-40 cm) since the thickness measurements are recorded every $\sim$4 m. A routine is then applied to the filtered profile to select minima that are deeper than a certain threshold value. The procedure is the same as used in many other studies for the detection of sails from surface ice profiles (e.g. [26] and [19]). Values ranging from -5 m to -9 m can be used as thresholds for keel detection ([29], [4]). Here we assume a sail height to keel depth ratio of 4 [25]. In many studies by, e.g., [19] and [26] a sail height of 0.8 m is used as threshold value for the identification of sails. This gives a threshold value for the keel depth equal to -3.2 m. Since the EM-bird underestimates the real thickness of ridges by up to 50-60% [6], we finally choose a cut-off depth of -1.5 m. Moreover, two adjacent keels have to satisfy the Rayleigh criterion: the minima points must be separated by a point whose depth is less than half of the depth of the keel in order to be resolved as separate entity ([9], [28], [27]). An example of a final profile is shown in figure 2. The depth of the keels that are detected and shown in figure 2 are then multiplied by a factor of 2 in order to account for the systematic underestimation of the maximum draft by a factor of 2 due to the EM technique ([16], [6]).

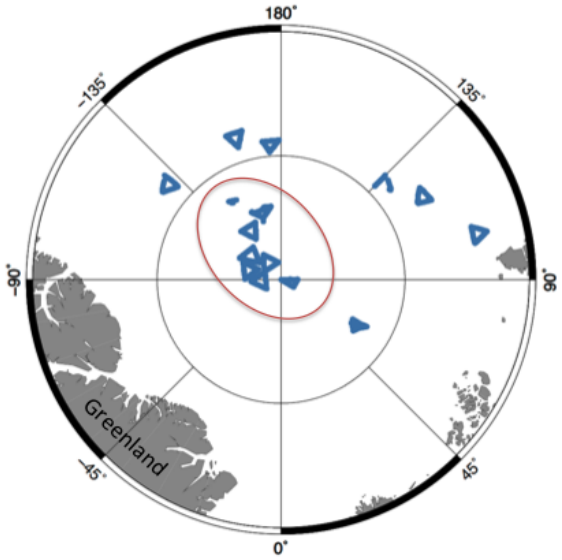

Fig. 1 Map of the Arctic Ocean with the location of the laser altimeter and EM-bird measurements. The red circle encloses the measurements taken in the area that in the present study is referred to as the Central Arctic.

3 Calculation of Oceanic Drag Coefficients

In order to calculate the oceanic drag coefficients we make use of a parameterization presented in [12]. This parameterization is based on a partitioning concept that was already introduced for atmospheric drag coefficients in [1] and [2]. The parameterization in [12] distinguishes between the influence of small scale roughness (skin drag) and larger obstacles such as the keels associated with ridges and the edges of the ice floes (form drag). Since we focus our analysis on areas with 100% sea-ice cover, the contribution of floe edges can be neglected.

The oceanic drag coefficient c_w is then the sum of the skin drag ${c_w}^s$ and the form drag due to ridges ${c_w}^r$:

$$c_w = {c_w}^s + {c_w}^r. \tag{1}$$

The drag contributions, in the case of sea-ice concentration A equal to 1, are calculated as following:

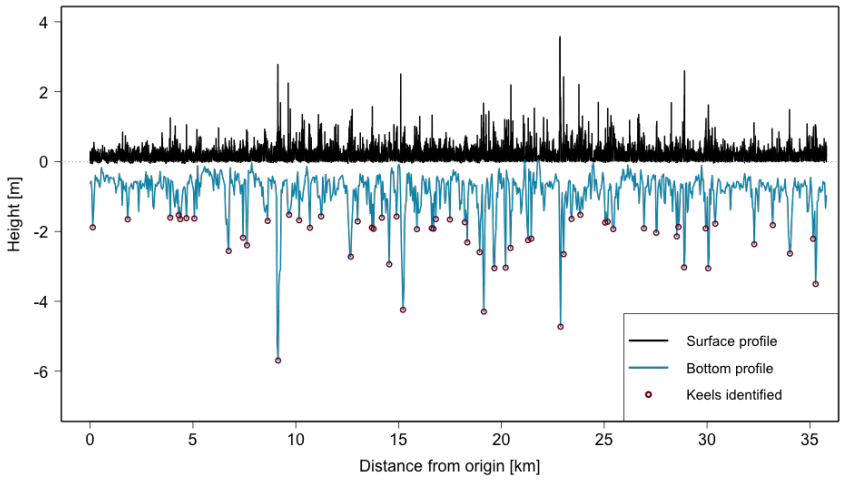

Fig. 2 An example of a sea ice profile of ca. 35 km length. The black line shows the upper surface profile obtained by the filtered laser altimeter data. The light blue line represents the bottom profile of the ice obtained by subtracting the thickness from the laser altimeter profiles. The circles represent the detected keels. The depth of the keels is then multiplied by a factor of 2 as described in section 2.

$$c_w{}^s = C_s \left(1 - m\frac{H_r}{D_r}\right), \tag{2}$$

$$c_w{}^r = \frac{C_r H_r}{\pi D_r}\left[1 - \left(\frac{H_r}{D_r}\right)^{1/2}\right]^2. \tag{3}$$

H_r and D_r are the mean depth of the keels and the mean separation between them respectively. The remaining constants are: $m = 1$, $C_r = 0.5$ and $C_s = 2 \times 10^{-3}$.

For the calculation of the drag coefficients we need to compute the mean depth of the keels H_r and the mean separation D_r between them as obtained from the available data. We focus on the Central Arctic region (see figure 1). There, we have 320 profiles. The length of each profile varies between ca. 10 km and 30 km for a total of more than 700 km of data. For each profile we detect the keels as described in section 2 and we calculate the mean depth and the mean spacing between them. With this information we can calculate the drag coefficients for each profile. The results are shown in figure 3.

Only a few measurements of oceanic drag coefficients are available for comparing the results obtained with equations 2 and 3. [12] showed (see their Table 1) that oceanic drag coefficients can vary from 1×10^{-3} to even 22×10^{-3}. Our calculated values lie within this range. We stress that the oceanic drag coefficients vary strongly with the sea-ice topography and that the choice of a constant value used in global

circulation models might imply a bias in the estimation of the momentum exchange between the ice and the ocean.

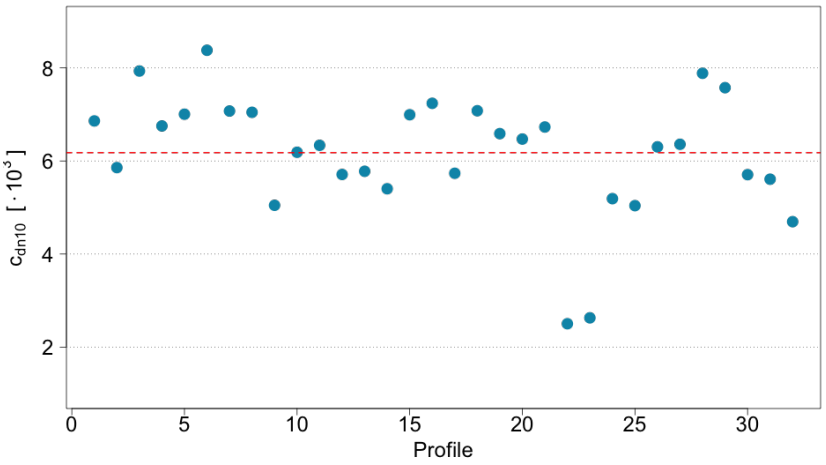

Fig. 3 Values of the oceanic drag coefficients c_w calculated for the Central Arctic. The red line represents the mean value.

4 Ekman pumping

Ekman pumping in the ocean depends on the spatial variation of the stress applied at the surface. This spatial variation is a consequence of variations in both the velocity field and the drag coefficients. In this section we want to evaluate the contribution to the Ekman pumping that is caused only by variations of the drag coefficients. We thus set up a very simple experiment. 32 grid cells aligned along y, each 20 km wide, form a domain of 20 km $\times$ 640 km. This domain is covered completely with sea ice (100 % sea-ice cover). The surface and bottom properties of the ice are varying from one cell to the other, so that the drag coefficients are also different. In particular, to each grid cell we assign a value for the drag coefficient that was calculated (see section 3) on the basis of real sea-ice topography. We assume that the ice is in motion along x with a constant velocity $v_{\mathrm{ice}} = 0.05$ m/s while the ocean is at rest. We then compute the Ekman pumping with:

$$w_{\mathrm{E}} = \hat{z} \cdot \nabla \times \frac{\tau}{\rho_0 f}, \tag{4}$$

where ρ_0 is the mean density of the sea water, τ is the stress at the surface, f is the Coriolis parameter. The stress term τ is given by:

$$\tau = \rho_0 c_w |\mathbf{v}_{\text{ice}}| \mathbf{v}_{\text{ice}}. \tag{5}$$

The formulation (equation 4) of the Ekman vertical velocity is only valid for large domains in a steady state and our 20 km grid axes may be too small. Nevertheless we can use such a simplified formulation because we are not primarily interested in quantifying the Ekman pumping, but we would like to illustrate the importance of variations in the value of oceanic drag coefficients alone on the Ekman pumping. The results of our calculations are shown in figure 4. In this simple experiment there would not be Ekman pumping if the drag coefficient were constant in the whole domain. The range of variations of the vertical velocity is between -20 cm/day and 30 cm/day. Simulated variations in the Ekman vertical velocity based on variations of the surface stress when no keels are taken into account are shown in [18] (their figure 6): Here the range of variations of annual mean vertical velocities over different regions in the Arctic is between -5 cm/day and 3 cm/day. In [18] the variations in the ocean-surface stress are caused by variations only in the wind field and not by variations in the drag coefficients. In our study we see a much higher variation than in [18] but we stress once more that their result shows variations averaged over the entire basin while here we focus on local variations.

From the results of this calculation we can conclude that the variations in Ekman pumping associated with variable oceanic drag coefficients is at least in the same order of magnitude as the variations due to changes in the surface velocity of the ice. Even though the strong local effect might be damped when averages are taken over a larger area, we can still assume that the effect will remain of the same order of the velocity variations shown by [18]. Thus we speculate that the presence of different sea-ice regimes on a large scale may induce a basin-scale variation in Ekman pumping that then would have consequences for the Ekman transport and the large scale ocean circulation. Numerical experiments and simulations with large scale sea ice-ocean models could help to investigate the effect on an Arctic basin scale ocean circulation.

5 Summary and Conclusion

Airborne altimetry and EM-bird observations have been used in the present study to reconstruct the surface and bottom topography of the sea-ice.

From the obtained profiles we detected the keels and calculated keel mean depth and keel mean separation along profiles of different length. This information is then used to calculate the oceanic drag coefficients. These coefficients are calculated by applying a parameterization presented in [12] to a hypothetical situation of 100% sea-ice cover. The calculated drag coefficients are in the range of values obtained by in-situ observations. The range of variability is large and this suggests that the choice

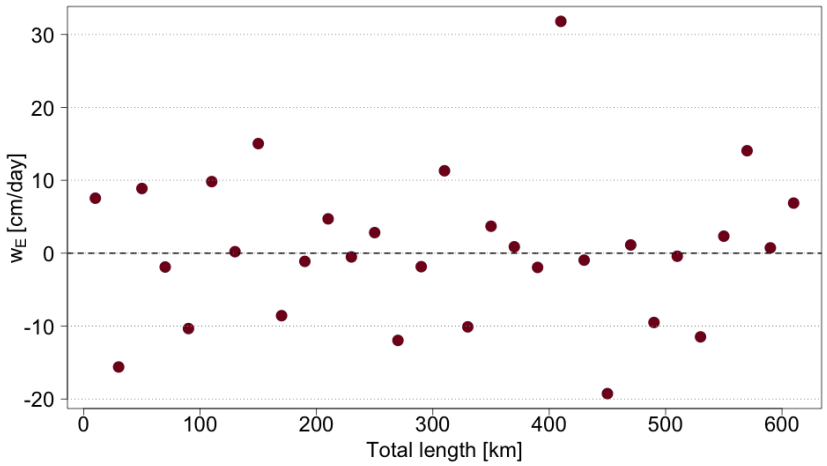

Fig. 4 Ekman pumping calculated for the idealized situation described in section 4.

of a constant drag in sea-ice numerical models might lead to a misrepresentation of the actual ice-ocean momentum transfer.

The calculated oceanic drag coefficients have been used for a rough calculation of Ekman pumping. The results provide an insight into the expected magnitude of Ekman pumping caused by the variability of the oceanic drag coefficients. The upper layer vertical velocity generated by variations in drag coefficients is on the same order of magnitude as for variable ice velocity at the surface. In order to better understand the importance of the variable drag coefficients on the large scale oceanic circulation, Pan Arctic simulations with global circulation models are required. The results shown here suggest that neglecting the contribution of variable oceanic drag coefficients in the momentum transfer between ice and ocean can lead to considerable errors in numerical models or data analysis.

Aknowledgments

We would like to thank the crew of the RV Polarstern and the HeliService International Gmbh. Moreover we thank all the people who contributed to collect the laser altimeter data and EM-bird data, in particular Stefan Hendricks. We are also very thankful to Michael Karcher for the interesting and constructive discussions. Finally we thank the Earth System Science Research School (ESSReS) for any support to this study and to the PhD project.

References

1. Arya S. P. S. 1973. Contribution of Form Drag on Pressure Ridges to the Air Stress on Arctic Ice. *J. Geophys. Res.*, **78**, No 30, 7092-7099.
2. Arya S. P. S. 1975. A Drag Partitioning Theory for Determining the Large-Scale Roughness Parameter and Wind Stress on the Arctic Pack Ice. *J. Geophys. Res.*, **80**, No 24, 3447-3454.
3. Birnbaum G. and C. Lüpkes. 2002. A new parameterization of surface drag in the marginal sea ice zone. *Tellus, 54A*, pp. 107-123.
4. Davis N. and P. Wadhams. 1996. A statistical analysis of Arctic pressure ridge morphology. *J. Geophys. Res. 100*, pp. 10,915-10,925.
5. Garbrecht, T., C. Lüpkes, J. Hartman and M. Wolf. 2002. Atmospheric drag coefficients over sea ice - validation of a parameterization concept. *Tellus*, **54A**, 205-219.
6. Haas C. 2004. EM ice thickness measurements during GreenICE 2004 field campaign, *Tech. rep.*, EU project GreenICE (EVK2-2001-00280), Alfred Wegener Institute, Bremerhaven, Germany.
7. Haas C., J. Lobach, S. Hendricks, L. Rabenstein and A. Pfaffling. 2009. Helicopter-borne measurements of sea ice thickness, using a small and lightweight, digital EM system. *J. Appl. Geophys., 67*, pp. 234-241.
8. Hibler III W.D., 1972. Removal of aircraft altitude variation from laser profiles of the Arctic pack. *Journal of Geophysical Research*, **77**, 36, 7190-7195.
9. Hibler W. D. III. 1975. Characterization of cold-regions terrain using airborne laser profilometry. *J. Geophys. Res., 77(36)*, pp. 7190-7195.
10. Kovacs, A., Holladay, J., and Bergeron, C., Jr. 1995. The footprint altitude ratio for helicopter electromagnetic sounding of sea-ice thickness: Comparison of theoretical and fiels estimates. *Geophysics, 60(2)*, pp. 374380. doi:10.1190/1.1443773.
11. Kovacs, A., Holladay, J., and Bergeron, C., Jr. 1995. The footprint altitude ratio for helicopter electromagnetic sounding of sea-ice thickness: Comparison of theoretical and fiels estimates. *Geophysics, 60(2)*, pp. 374380. doi:10.1190/1.1443773.
12. Lu P., Z. Li, B. Cheng and M. Leppäranta. 2011. A parameterization of the ice-ocean drag coefficient. *Journal of Geophysical Research*. **116**, C07019.
13. Lüpkes, C. and G. Birnbaum. 2005. Surface drag in the Arctic marginal sea-ice zone: a comparison of different parameterisation concepts. *Boundary-Layer Meteorology*, **117**, pp. 179-211, doi:10.1007/s10546-005-1445-8.
14. Lüpkes, C., V. M. Gryanic, J. Hartmann and E. L. Andreas. 2012. A parameterization, based on sea ice morphology, of the neutral atmospheric drag coefficients for weather prediction and climate models. *Journal of Geophysical research* **117**, D13112
15. Lüpkes C., V. Gryanic, A. Rösel, G. Birnbaum, L. Kaleschke. 2013. Effects of sea ice morphology during arctic summer on atmospheric drag coefficients used in climate models. *Geophsy. Res. Lett.*, doi:10.1029/2012GL054354, in press.
16. Martin, T. (2007) Arctic Sea Ice Dynamics: Drift and Ridging in Numerical Models and Observations., PhD thesis *Ber. Polarforsch. Meeresforsch.*, **563**, ISSN 1618-3193.
17. Pite H. D., D. R. Topham and J. V. Hardenberg. Laboratory Measurements of the Drag Force on a Family of Two-Dimensional Ice Keel Models ina Two-Layer Flow. *Journal of Physical Oceanography*, **25**, pp. 3008-3031.
18. Rabe, B., M. Karcher, U. Schauer, J. M. Toole, R. A. Krishfield, S. Pisarev, F. Kauker, R. Gerdes, T. Kikuchi. 2011. An assessment of Arctic Ocean frashwater content changes from the 1990s to the 2006.2008 period. *Deep Sea Research Part I: Oceanographic Research Paper*, **58**, 2, pp. 173-185.
19. Rabenstein L., S. Hendricks, T. Martin., A. Pfaffhuber and C. Haas. 2010. Thickness and surface-properties of different sea-ice regimes within the Arctic Trans Polar Drift: Data from summers 2001, 2004 and 2007. *J. Geophys. Res., 115*, doi:10.1029/2009JC005846
20. Redi J., A. Pfaffling and M. Vrbancich. 2006. Airborne electromagnetic footprints in 1D earths., *Geophysics, 71*, G63-G72

21. Steele, M., J. H. Morison, and N. Untersteiner. (1989) The partition of air-ice-ocean momentum exchange as a function of ice concentration, floe size, and draft. *J. Geophys. Res.*, **94**, C9, pp. 12,739-12,750.
22. Steiner N., M. Harder, P. Lemke. 1999. Sea-ice roughness and drag coefficients in a dynamic-thermodaynamic sea-ice model for the -arctic. *Tellus*, **51A**, 964-978.
23. Steiner N. 2000. Introduction of variable drag coefficients insto sea-ice models. *Annals of Glaciology*, 33, pp. 181-186
24. Thorndike A.S. and R. Colony. 1982. Sea ice motion in response to geostrophic winds. emphJ. Geophys. Res., 87, pp. 5845-5852.
25. Timco M. and R. P. Burden. 1997. An analysis of the shape of sea ice ridges. *Cold Reg. Sci. Technol., 25*, pp. 65-77.
26. Von Saldern C., C. Haas, W. Dierking. 2006. Parameterization of Arctic sea-ice surface roughness for application in ice type classification. *Annals of Glaciology*, 44, pp. 224-230
27. Wadhams P. and R. Horne. 1980. An analysis of ice profiles obtained by submarine sonar in the Beaufort Sea, *J. Glaciol., 25*, pp. 401-424.
28. Wadhams P. and T. Davy. 1986. On the spacing and draft distributions for pressure ridges keels. *J. Geophys. Res., 91*, pp. 10,697-10,708, doi:10.1029/JC09p10697.
29. Williams E., C. Swithinbank and G. de Q. Robin. 1975. A submarine sonar study of Arctic pack ice. *J. Glaciol., 15(73)*, pp. 349-362.